Biomechanical Impact of Wrong Positioning of a Dedicated Stent for Coronary Bifurcations: A Virtual Bench Testing Study

Biomechanical impact of wrong positioning of a dedicated stent for coronary bifurcations: A virtual bench testing study

Claudio Chiastra[1]*, Maik J. Grundeken[2]*, Carlos Collet[2,3], Wei Wu[1,4], Joanna J. Wykrzykowska[2], Giancarlo Pennati[1], Gabriele Dubini[1], Francesco Migliavacca[1]

1. Laboratory of Biological Structure Mechanics (LaBS), Department of Chemistry, Materials and Chemical Engineering "Giulio Natta", Politecnico di Milano, Milan, Italy
2. The Heart Center, Academic Medical Center – University of Amsterdam, Amsterdam, The Netherlands
3. Department of Cardiology, Universitair Ziekenhuis Brussel, Brussel, Belgium
4. Department of Mechanical Engineering, University of Texas at San Antonio, San Antonio, Texas, USA

* C. Chiastra and M.J. Grundeken contributed equally.

Address for correspondence:

Dr. Claudio Chiastra, PhD

Laboratory of Biological Structure Mechanics (LaBS)

Department of Chemistry, Materials and Chemical Engineering "Giulio Natta"

Politecnico di Milano

Piazza Leonardo da Vinci 32

20133 Milan, Italy

Tel.: +39 02 2399 4283

E-mail: claudio.chiastra@polimi.it

ORCID: http://orcid.org/0000-0003-2070-6142

Abstract

The treatment of coronary bifurcations is challenging for interventional cardiologists. The Tryton stent (Tryton Medical, Inc., USA) is one of the few devices specifically designed for coronary bifurcations that underwent large clinical trials. Although the manufacturer provides specific recommendations to position the stent in the bifurcation side branch (SB) according to four radio-opaque markers under angiographic guidance, wrong device positioning may accidentally occur. In this study, the virtual bench testing approach was used to investigate the impact of wrong positioning of the Tryton stent in coronary bifurcations in terms of geometrical and biomechanical criteria.

A finite element model of the left anterior descending / first diagonal coronary bifurcation was created with a 45° distal angle and realistic lumen diameters. A validated model of the Tryton stent mounted on stepped delivery balloon was used. All steps of the Tryton deployment sequence were simulated. Three Tryton positions, namely 'proximal', 'recommended', and 'distal' positions, obtained by progressively implanting the stent more distally in the SB, were compared.

The 'recommended' case exhibited the lowest ostial area stenosis (44.8% vs. 74.3% ('proximal') and 51.5% ('distal')), the highest diameter at the SB ostium (2.81mm vs. 2.70mm ('proximal') and 2.54mm ('distal')), low stent malapposition (9.9% vs. 16.3% ('proximal') and 8.5% ('distal')), and the lowest peak wall stress (0.37MPa vs. 2.20MPa ('proximal') and 0.71MPa ('distal')).

In conclusion, the study shows that a 'recommended' Tryton stent positioning may be required for optimal clinical results.

Keywords

Interventional cardiology, coronary bifurcation, stent, numerical models, finite element analysis

Introduction

Atherosclerotic lesions at coronary bifurcations represent the 15-20% of the coronary artery lesions observed in patients undergoing cardiac catheterization.[23] Their treatment is a challenge for interventional cardiologists resulting in lower procedural success rate and higher risk of long-term cardiac events as compared to non-bifurcated segments.[23] Over the last decade, many stents specifically designed for coronary bifurcations have been developed. However, most of them remained prototypes and are not used in routine clinical practice. The Tryton Side Branch stent (Tryton Medical, Inc., Durham, NC, USA) is one of the few dedicated devices that underwent large clinical trials.[17,23] The Tryton bifurcation trial compared the Tryton stent (used in combination with a drug-eluting stent in the main branch, MB) against drug-eluting stent placement in the MB in combination with side branch (SB) balloon dilatation. The primary end-point of the trial (a combined endpoint of cardiac death, target-vessel myocardial infarction, and target-vessel revascularization) was not met due to a higher amount of peri-procedural myocardial infarction in the Tryton arm.[12] A post-hoc subgroup analysis of this trial suggested that this was caused by an increased incidence of peri-procedural myocardial infarction in patients with bifurcation lesions with SBs < 2.5 mm (which was a formal exclusion criterion).[11] Indeed, a confirmatory study[13] including only patients with large SBs > 2.5 mm reached its pre-specified performance goal (which was based on the peri-procedural myocardial infarction rate in the single-stent group of the Tryton bifurcation trial), and this study led to Food and Drug Administration (FDA) approval for its use in the USA in 2017, after it already had received a CE mark in 2008 for clinical use in Europe. A post-market study has been launched and the stent is used in daily clinical practice to treat bifurcation lesions; therefore, a better understanding of its mechanical behavior is of great importance for the interventional cardiologists.

The Tryton stent is designed to be deployed in the SB of coronary bifurcations (Fig. 1, panel A).[15]

Unlike the conventional state-of-the-art coronary stents, the Tryton stent is characterized by fewer struts in its proximal portion to facilitate the implantation of an additional stent in the MB.[15] The Tryton stent is positioned according to four radio-opaque markers under angiographic guidance. The manufacturer recommends deploying the stent so that the bifurcation carina is positioned 1/3 the distance from the distal middle marker (Fig. 1, panel A). However, the potential foreshortening of the coronary bifurcation in the 2D angiographic images (i.e. the misrepresentation of the true lengths of the bifurcation branches occurring when the X-ray beam is not aligned perpendicularly to the vessel) and the movements of the device during the cardiac cycle make the positioning of the Tryton stent challenging. The deployment of the stent in a wrong position may accidentally occur. As an example, in Fig. 1 a clinical case with correct positioning is compared against one with incorrect positioning. The angiographic images and 3D optical coherence tomography (OCT) reconstructions show that in the first patient the manufacturer recommendations for correct deployment were followed (Fig. 1, panels B, D, F) while in the second one the stent was positioned too proximally (Fig. 1, panels C, E, G).

Modeling techniques of stent deployment based on the finite element analysis have emerged as powerful tools for the assessment of geometrical and mechanical variables that are hardly detectable *in vitro* or *in vivo*.[1,25] The present study investigates the impact of wrong positioning of the Tryton stent in coronary bifurcations in terms of geometrical and biomechanical criteria by using a virtual bench testing approach.

Material and methods

Coronary bifurcation model

A finite element model of one of the main coronary bifurcations (i.e. left anterior descending coronary artery with its first diagonal branch) was created (Fig. 2A). The geometry is characterized by

a distal bifurcation angle of 45° and a proximal-to-distal MB angle of 180°.[5] The lumen diameters were defined within the physiological range for this specific coronary bifurcation[24] and obeyed the Finet's law[8], which establishes a relationship between the proximal MB lumen diameter and the distal MB and SB lumen diameters. The vessel wall thickness was set as the 30% of the lumen diameters according to experimental tests on human coronary artery specimens.[20] The vessel wall accounted for its three typical layers (i.e. intima, media, adventitia) with thicknesses measured *ex vivo* by Holzapfel et al.[20] An isotropic hyperelastic constitutive law based on a reduced polynomial strain energy function of sixth order was used to describe the material behavior of each layer, as previously done.[26,27] The material density was set to 1120 kg/m^3.[10] The vessel wall model was discretized using ~132,000 eight-node cubic elements (2 layers of elements for each vessel wall layer[27], Fig. 2A). The software SolidWorks (Dassault Systèmes SolidWorks Corp., Waltham, MA, USA) and ICEM CFD (ANSYS Inc., Canonsburg, PA, USA) were used to create the geometry and the mesh of the bifurcation model, respectively.

Tryton stent model

The Tryton stent has a cobalt-chromium platform with a strut thickness of 84 μm.[15,17] It is built in a single rapid exchange delivery system with four radio-opaque markers to guide positioning. The stent is balloon-expandable and mounted on either a straight or a stepped delivery balloon. The stent consists of three zones, namely proximal, central, and distal zones.[15,17] The proximal MB zone has two 'wedding bands' on the stent's proximal edge, which mount the stent on the delivery balloon and 'anchor' the stent in the proximal MB after implantation. From the 'wedding bands', three undulating fronds emerge, which connect the 'wedding band' with the panels of the transition zone. The central transition zone is built from three panels, which can be independently deformed to accommodate to a wide range of carinal anatomy. The special design of these panels provides both optimal scaffolding

and coverage of the SB ostium, provided that the stent positioning is done properly according to the markers. The distal SB zone has the standard design of a conventional tubular stent with four circumferential out-of-phase zigzag hoops linked together by one or two (depending on stent size) connectors in-between the subsequent hoops. The distal SB zone is smaller than the proximal MB zone (except for the straight model), with SB diameters ranging from 2.5 to 3.5 mm and MB diameters ranging from 3.0 to 4.0 mm. This difference in diameters accommodates the fractal geometry of the coronary tree, in which there is a natural step-down in vessel diameter at each branching point (i.e. bifurcation).[18]

A previously validated model of a Tryton stent (length of 19 mm, mounted on a stepped delivery balloon of 2.5 - 3.5 mm) was used (Fig. 2B, top).[3] Briefly, the stent geometry was created in its crimped configuration from stereomicroscope images of a Tryton stent sample by means of SolidWorks (Dassault Systèmes SolidWorks Corp., Waltham, MA, USA). The stent material was described using a Von Mises-Hill plasticity model with isotropic hardening.[3] The following material properties were assigned to the model: Young's modulus of 233 GPa, Poisson's ratio of 0.35, yield stress of 414 MPa, ultimate stress of 933 MPa, deformation at break of 44.5%, and density of 8,000 kg/m^3. The stent geometry was discretized with ~68,000 eight-node cubic elements using HyperMesh (Altair Engineering, Troy, MI, USA) (Fig. 2C, left). The polymeric material of the delivery balloon was modeled using a linear elastic isotropic constitutive law. To replicate the manufacturer's pressure-diameter curve, Young's moduli of 400 MPa and 388 MPa, which were derived after a calibration procedure, were assigned to the proximal and distal balloon portions, respectively.[3] A Poisson's ratio of 0.45 was chosen.[3] The material density was set to 1,000 kg/m^3. The stepped balloon geometry was meshed with ~15,000 four-node membrane elements with reduced integration using HyperMesh.

Conventional stent and balloon angioplasty models

In addition to the Tryton stent, the model of a 3×15 mm conventional drug-eluting stent Xience V (Abbott Laboratories, Abbott Park, IL, USA) with strut thickness of 81 μm, was used (Fig. 2B, bottom). The Xience V stent was selected for this study because it is considered as one of the best-of-class drug-eluting stent with a robust body of evidence supporting its efficacy and safety. The cobalt-chromium alloy that characterizes this stent was modeled using the same constitutive law and material properties adopted for the Tryton stent material. The stent geometry was meshed with ~251,000 eight-node reduced integration cubic elements (Fig. 2C, right). Element size was chosen according to previous grid sensitivity analyses[2,26] and is comparable or finer to that reported in other studies where the Xience stent was modeled.[33,34] Additional details about this stent model can be found in a previous study.[26]

A multi-folded, unexpanded model of the NC Sprinter RX non-compliant balloon (Medtronic, Fridley, MN, USA) was also created using SolidWorks. Different balloon sizes (i.e. 2×15 mm, 3×15 mm, and 3.5×9 mm) were modeled according to the procedural steps of the Tryton stent implantation. The balloon thickness was 25 μm.[4] The polymeric material of the balloon was considered to be linear elastic and isotropic. Likewise done with the Tryton stepped balloon, the Young's modulus was chosen after a calibration procedure so that the pressure-diameter curve obtained with the balloon model matches that provided by the manufacturer. The following values were found depending on the different balloon sizes: 217 MPa for the 2.5×15 mm balloon, 287 MPa for the 3×15 mm balloon, and 327 MPa for the 3.5×9 mm balloon. The Poisson's ratio was set to 0.45 and the material density to 1,000 kg/m^3.[4] 9,000, 4,600, and ~7,300 four-node membrane elements with reduced integration were used to discretize the 2×15 mm, 3×15 mm, and 3.5×9 mm balloons, respectively, by means of HyperMesh.

Virtual bench testing simulations

The Tryton deployment sequence, known as Tryton-based culotte technique, was simulated using the finite element solver ABAQUS/Explicit (Dassault Systèmes Simulia Corp., Providence, RI, USA). As recommended in the instruction for use provided by the Tryton stent manufacturer, the following procedural steps were simulated (Fig. 3)[14]:

1) Tryton stent deployment: insertion of a 2.5, 3.5×19 mm Tryton stent in the SB (Fig. 3A); stent expansion at 10 atm (Fig. 3B); stent release;
2) Proximal optimization technique: expansion of a 3.5×9 mm NC Sprinter RX balloon at 8 atm in the proximal MB to ensure adequate apposition of the Tryton 'wedding bands' to the vessel wall (Fig. 3C);
3) Opening of the MB access: expansion of a 3×15 mm NC Sprinter RX balloon at 8 atm in the MB through the Tryton stent struts to pre-dilate the distal MB and facilitate the subsequent MB stent delivery (Fig. 3D);
4) Xience V stent deployment: expansion of a 3×15 mm Xience V stent at 9 atm in the MB (Fig. 3E);
5) Kissing balloon inflation: simultaneous expansion of a 2.5×15 mm and 3×15 mm NC Sprinter RX balloon at 8 atm in the SB and MB, respectively (Fig. 3F);
6) Proximal optimization technique: expansion of a 3.5×9 mm NC Sprinter RX balloon at 9 atm to reduce the oval-shaped stent distortions in the proximal MB that are created by the overlap of the kissing balloons in the proximal MB (Fig. 3G,H).

Each procedural step was considered as a separate finite element analysis to reduce the computational efforts. The deformed geometries obtained at the end of each simulated step as well as their corresponding stress and deformation state were imported from each analysis to the subsequent one. All procedural steps were simulated as quasi-static processes by maintaining the ratio between

kinetic and internal energy below 5% during the entire simulation.[27] The general contact algorithm available in ABAQUS/Explicit was chosen to define the contacts between parts of the model with 'hard' normal behavior and tangential behavior with static friction coefficient of 0.2.[27–29] As boundary conditions, the nodes of the vessel wall extremities were constrained in the circumferential and radial directions.[27] Similarly to previous studies[4,14,21,26,27], preliminary finite element analyses were performed to bend the Tryton stent, its stepped delivery balloon, and the 2.5×15 mm NC Sprinter RX balloon, and allow for their correct positioning in the SB. Cylindrical surfaces were used to bend those models under displacement control.

Three different scenarios were compared by means of the virtual bench testing simulations:

- 'Proximal' Tryton stent positioning: the distal end of the central Tryton stent zone is placed precisely at the level of the carina (Fig. 4, top);
- 'Recommended' Tryton stent positioning: the Tryton stent is placed so that the carina is positioned 1/3 the distance from the distal middle marker (Fig. 4, centre);
- 'Distal' Tryton stent positioning: the Tryton stent is placed so that the carina is at 2/3 from the distal middle marker, instead of 1/3 (Fig. 4, bottom).

To compare the three scenarios, both geometrical and mechanical variables were computed. In particular, geometrical quantities such as the distal bifurcation angle change induced by the stent deployment, the SB ostial area stenosis, the Tryton stent diameter at the SB ostium and the stent strut malapposition were evaluated at the end of the stenting procedure. The SB ostial area stenosis was calculated as[32]: (total SB ostium area – largest area free from struts) / total SB ostium area * 100. The stent malapposition was quantified as the percent area of struts not in contact with the lumen (i.e. malapposed struts) with respect to the total area of the abluminal stent surface. A threshold of 130 μm was used to discriminate between the struts in contact / not in contact with the lumen, as previously done in an *in vitro* bench test analysis.[7] A mechanical quantity, the arterial wall stress, was analysed

after stenting implantation.

Results

The three scenarios under investigation were compared in terms of geometrical and mechanical quantities. The stenting procedure decreased the distal bifurcation angle in all cases (Fig. 4B, Table 1). The more distal the Tryton stent was placed, the larger bifurcation angle change occurred.

The cross-sectional view of the SB ostium is shown in Fig. 5 for all investigated cases. The SB ostial area stenosis, which is indicated in yellow in the figure, was evaluated to assess the SB opening. The values of SB ostial area stenosis are reported in Table 1 for the three cases. The 'recommended' case was the best scenario as it exhibited the lowest SB ostial area stenosis. On the contrary, the 'proximal' case presented the highest and, hence, the worst SB ostial area stenosis.

Figure 6 shows the Tryton stent diameter at the SB ostium. The 'recommended' Tryton positioning was characterized by the highest diameter. As highlighted by the stent lateral view in Fig. 6, in the 'proximal' and 'distal' scenarios the Tryton stent was slightly squeezed after implantation at the bifurcation region, resulting in a smaller diameter at the SB ostium than the 'recommended' case.

Stent malapposition is presented in Fig. 7. In all cases, malapposed struts (indicated in red in Fig. 7) were mainly confined at the stent lateral portions in the proximal MB. The 'proximal' case had the highest percentage of malapposed struts as compared to other two cases (Table 1).

Finally, Fig. 8 displays the arterial wall stress in the three investigated cases after stenting implantation. In all scenarios, high values of maximum principal stress were found at the proximal MB. The peak stress was located at the proximal MB next to the SB ostium, opposite to the carina. The 'proximal' Tryton positioning resulted in larger areas with high stress at the proximal MB, as compared to the other scenarios. Moreover, it was associated with the highest peak stress (Table 1). Conversely,

the 'recommended' scenarios exhibited the lowest peak stress (Table 1).

Discussion

The present virtual bench testing study demonstrated that: 1) The 'recommended' positioning of the dedicated bifurcation Tryton stent resulted in the lowest ostial area stenosis and highest luminal diameter at the SB ostium, lower stent malapposition and lowest peak arterial wall stress compared to a 'proximal' and 'distal' stent positioning; 2) the 'proximal' positioning was associated with the highest area stenosis, malapposition and peak wall stress, whereas 'distal' positioning induced the smallest luminal diameter at the SB ostium.

Dedicated bifurcation stent systems were developed to assist the interventional cardiologists in the percutaneous treatment of bifurcation lesions. The design of the Tryton stent aimed to preserve SB patency while facilitating the percutaneous coronary intervention (PCI) technique.[17] A randomized clinical trial comparing the efficacy of the Tryton stent system with a conventional "provisional" strategy (i.e. implantation of a drug-eluting stent in the MB with additional SB balloon dilatation[22]) failed to show non-inferior clinical outcomes of the Tryton stent at 9-month follow-up.[12] The rate of the primary endpoint (composite of cardiac death, target vessel myocardial infarction and clinically indicated target vessel revascularization) was 17.4% with Tryton and 12.8% with the provisional strategy (difference +4.6%; p-value for non-inferiority=0.42). In addition, despite being specifically designed for the bifurcation SB, no difference was found in the percent diameter stenosis, assessed by dedicated bifurcation quantitative coronary angiography, compared to balloon dilatation at 9-month follow-up angiography.[16]

Hitherto, a detailed analysis of the position of the Tryton stent in the SB and its correlation with clinical outcomes is lacking. From the PCI technique standpoint, the precise positioning of the device is

challenging due to the potential foreshortening of the bifurcation in the 2D angiographic images and the continuous movement of the device during the cardiac cycle. Therefore, an accurate positioning, as the manufacturer recommends, may be difficult to achieve in clinical practice. In the present study, the effects of the positioning of the Tryton stent in terms of geometrical and biomechanical aspects were investigated by means of virtual bench simulation of the culotte stenting technique and three stent positions. The 'recommended' positioning of the Tryton stent resulted in the lowest ostial area stenosis at the SB and lower malapposed struts. Stent struts at the SB orifice have been associated to thrombus attachment.[19] Moreover, strut malapposition has been associated with platelet activation and stent thrombosis.[30] In this study, the 'proximal' positioning of the Tryton stent resulted in the highest proportion of malapposed struts compared to the 'recommended' and 'distal' positioning (16.3% vs. 9.9% and 8.5% for the 'recommended' and 'distal' cases). In line with previous clinical studies assessing strut malapposition with OCT after Tryton stent implantation, the longitudinal distribution of malapposed struts showed to be higher in the bifurcation region than in both proximal and distal segments. Interestingly, Tyczynski et al.[37] reported a total percent of malapposed struts of 18.1%, which is comparable to the malapposition rate found with the 'proximal' positioning; however, here a detailed analysis of the Tryton stent positioning was lacking. Overall, the favorable results observed with the simulation of 'recommended' positioning reinforce the importance of adequate device positiong.

In-stent restenosis after bifurcation stenting is most commonly focal and located at the SB ostium. Stent underexpansion at this location has shown to be the dominant mechanism of restenosis after bifurcation PCI.[6] The simulation of the 'proximal' and 'distal' Tryton position showed lower luminal diameter at the ostium of the SB as compared with the 'recommended' scenario. Moreover, stent underexpansion has been shown to promote areas of low endothelial shear stress, to increase the amount of neointimal hyperplasia and in-stent restenosis.[9,36] Furthermore, wrong positioning of the

Tryton stent resulted in higher arterial wall stress with a peak at the ostium of the SB location, which has shown to correlate with restenosis after bare-metal stent implantation.[35]

The consensus document on bench testing for coronary artery bifurcation from the European Bifurcation Club highlights the usefulness of bench testing to assess stent deployment quality, SB access and correction of stent distortion.[31] The virtual bench simulations of PCI in bifurcation lesions, which are based on computer simulations, are complementary to the traditional *in vitro* bench testing.[25] Moreover, virtual bench simulations have the potential to increase our understanding of structural and hemodynamic alterations produced by stenting and even aid the interventional cardiologists guiding the interventional strategy and treatment planning in these subsets of lesions.[1,25] Our group has previously demonstrated the accuracy of a virtual bench simulation of the Tryton stent deployment in bifurcation lesions.[26] The findings of the present study highlight the importance of stent positioning and potential mechanical mechanism of stent failure. They raise awareness of the importance of the 'recommended' Tryton position to achieve adequate diameter at the SB ostium, low stent malapposition and low peak arterial wall stress, which may have a positive impact on clinical outcomes.

The study is based exclusively on finite element analyses of stent deployment in a population-based coronary bifurcation model with a distal bifurcation angle of 45°, proximal-to-distal MB angle of 180°, and without plaques. The bifurcation model does not include anisotropic, inhomogeneous arterial wall layers. Since the virtual bench testing approach allows the quantification of geometrical and mechanical variables by varying one specific bifurcation component at a time, further computational analyses might be conducted to investigate the impact of the bifurcation angle or atherosclerotic plaques (by analyzing different plaque locations and compositions) on the Tryton stent positioning from the biomechanical viewpoint. Furthermore, finite element analyses of stent deployment might be performed to quantify the biomechanical impact of other procedural aspects of the Tryton-based culotte technique. For instance, a recent study investigated the impact on stent geometry and mechanics of

rewiring through one of the panels of the Tryton stent instead of the re-wiring in-between the stent panels.[14] Also the impact of the orientation of the devices deserves further investigation.

To confirm the findings of the present study, the Tryton stent position and the quality of the stent deployment should be analyzed *in vivo* in a large population. It is difficult, however, to confirm the stent position with conventional imaging modalities (e.g. angiography). A more sophisticated analysis with 3D OCT, with the pullback taken from the SB after Tryton implantation (before MB stenting), may be necessary to further investigate the correlation of stent position and clinical outcomes.

Conclusions

In the present study, virtual bench simulations were performed to investigate the impact of the different positioning of the Tryton stent in a coronary bifurcation model in terms of geometrical and biomechanical aspects. Three different Tryton stent positions, namely 'proximal', 'recommended', and 'distal' positions, obtained by progressively implanting the stent more distally in the bifurcation SB, were compared. Overall, the 'recommended' Tryton stent positioning (i.e. the one suggested by the manufacturer) resulted in the best scenario as it exhibited the lowest ostial area stenosis (44.8%) and highest diameter at the SB ostium, lower stent malapposition, and the lowest peak arterial wall stress. The 'proximal' positioning was the worst scenario with the highest ostial area stenosis (74.3%), malapposition, and peak arterial wall stress. The 'distal' positioning was associated with the smallest luminal diameter at the SB (2.54 mm vs 2.81 mm in the 'recommended' position). These differences in ostial area stenosis and luminal diameter are likely to translate in differences in clinical outcomes (i.e. restenosis rates), especially when taking into account that the Tryton is a bare metal stent.

Acknowledgements

None.

Compliance with Ethical Standards

Conflict of Interest

The authors declare no conflicts of interest.

Ethical approval

All procedures performed in studies involving human participants were in accordance with the ethical standards of the institutional and/or national research committee and with the 1964 Helsinki declaration and its later amendments or comparable ethical standards. The clinical images reported in Fig. 1 were obtained during daily clinical routine (after the Tryton stent has received CE mark). The images used in Fig. 1 were retrieved from existing clinical database. Patients were not subject to additional (imaging) procedures other than clinical routine and thus written informed consent was not obtained. This article does not contain any studies with animals performed by any of the authors.

References

1. Antoniadis, A. P., P. Mortier, G. Kassab, G. Dubini, N. Foin, Y. Murasato, A. A. Giannopoulos, S. Tu, K. Iwasaki, Y. Hikichi, F. Migliavacca, C. Chiastra, J. J. Wentzel, F. Gijsen, J. H. C. Reiber, P. Barlis, P. W. Serruys, D. L. Bhatt, G. Stankovic, E. R. Edelman, G. D. Giannoglou, Y. Louvard, and Y. S. Chatzizisis. Biomechanical Modeling to Improve Coronary Artery Bifurcation Stenting: Expert Review Document on Techniques and Clinical Implementation. *JACC Cardiovasc. Interv.* 8:1281–96, 2015.
2. Capelli, C., F. Gervaso, L. Petrini, G. Dubini, and F. Migliavacca. Assessment of tissue prolapse after balloon-expandable stenting: influence of stent cell geometry. *Med. Eng. Phys.* 31:441–7, 2009.

3. Chiastra, C., M. J. Grundeken, W. Wu, P. W. Serruys, R. J. de Winter, G. Dubini, J. J. Wykrzykowska, and F. Migliavacca. First report on free expansion simulations of a dedicated bifurcation stent mounted on a stepped balloon. *EuroIntervention* 10:e1-3, 2015.

4. Chiastra, C., W. Wu, B. Dickerhoff, A. Aleiou, G. Dubini, H. Otake, F. Migliavacca, and J. F. LaDisa. Computational replication of the patient-specific stenting procedure for coronary artery bifurcations: From OCT and CT imaging to structural and hemodynamics analyses. *J. Biomech.* 49:2102–2111, 2016.

5. Collet, C., Y. Onuma, R. Cavalcante, M. Grundeken, P. Généreux, J. Popma, R. Costa, G. Stankovic, S. Tu, J. Reiber, J.-P. Aben, J. Lassen, Y. Louvard, A. Lansky, and P. Serruys. Quantitative angiography methods for bifurcation lesions: a consensus statement update from the European Bifurcation Club. *EuroIntervention* 13:115–123, 2017.

6. Costa, R. A., G. S. Mintz, S. G. Carlier, A. J. Lansky, I. Moussa, K. Fujii, H. Takebayashi, T. Yasuda, J. R. Costa Jr., Y. Tsuchiya, L. O. Jensen, E. Cristea, R. Mehran, G. D. Dangas, S. Iyer, M. Collins, E. M. Kreps, A. Colombo, G. W. Stone, M. B. Leon, and J. W. Moses. Bifurcation coronary lesions treated with the "crush" technique: an intravascular ultrasound analysis. *J Am Coll Cardiol* 46:599–605, 2005.

7. Derimay, F., G. Souteyrand, P. Motreff, G. Rioufol, and G. Finet. Influence of platform design of six different drug-eluting stents in provisional coronary bifurcation stenting by rePOT sequence: a comparative bench analysis. *EuroIntervention* 13:e1092–e1095, 2017.

8. Finet, G., M. Gilard, B. Perrenot, G. Rioufol, P. Motreff, L. Gavit, and R. Prost. Fractal geometry of arterial coronary bifurcations: a quantitative coronary angiography and intravascular ultrasound analysis. *EuroIntervention* 3:490–498, 2007.

9. Foin, N., J. L. Gutiérrez-Chico, S. Nakatani, R. Torii, C. V. Bourantas, S. Sen, S. Nijjer, R. Petraco, C. Kousera, M. Ghione, Y. Onuma, H. M. Garcia-Garcia, D. P. Francis, P. Wong, C. Di Mario, J. E. Davies, and P. W. Serruys. Incomplete stent apposition causes high shear flow disturbances and delay in neointimal coverage as a function of strut to wall detachment distance implications for the management of incomplete stent apposition. *Circ. Cardiovasc. Interv.* 7:180–189, 2014.

10. Gastaldi, D., S. Morlacchi, R. Nichetti, C. Capelli, G. Dubini, L. Petrini, and F. Migliavacca. Modelling

of the provisional side-branch stenting approach for the treatment of atherosclerotic coronary bifurcations: Effects of stent positioning. *Biomech. Model. Mechanobiol.* 9:551–561, 2010.

11. Généreux, P., A. Kini, M. Lesiak, I. Kumsars, G. Fontos, T. Slagboom, I. Ungi, D. C. Metzger, J. J. Wykrzykowska, P. R. Stella, A. L. Bartorelli, W. F. Fearon, T. Lefèvre, R. L. Feldman, G. Tarantini, N. Bettinger, G. Minalu Ayele, L. LaSalle, D. P. Francese, Y. Onuma, M. J. Grundeken, H. M. Garcia-Garcia, L. L. Laak, D. E. Cutlip, A. V Kaplan, P. W. Serruys, and M. B. Leon. Outcomes of a dedicated stent in coronary bifurcations with large side branches: A subanalysis of the randomized TRYTON bifurcation study. *Catheter. Cardiovasc. Interv.* 87:1231–41, 2016.
12. Généreux, P., I. Kumsars, M. Lesiak, A. Kini, G. Fontos, T. Slagboom, I. Ungi, D. C. Metzger, J. J. Wykrzykowska, P. R. Stella, A. L. Bartorelli, W. F. Fearon, T. Lefèvre, R. L. Feldman, L. LaSalle, D. P. Francese, Y. Onuma, M. J. Grundeken, H. M. Garcia-Garcia, L. L. Laak, D. E. Cutlip, A. V. Kaplan, P. W. Serruys, and M. B. Leon. A Randomized Trial of a Dedicated Bifurcation Stent Versus Provisional Stenting in the Treatment of Coronary Bifurcation Lesions. *J. Am. Coll. Cardiol.* 65:533–543, 2015.
13. Généreux, P., I. Kumsars, J. E. Schneider, M. Lesiak, B. Redfors, K. Cornelis, M. R. Selmon, J. Dens, A. Hoye, D. C. Metzger, L. Muyldermans, T. Slagboom, D. P. Francese, G. M. Ayele, L. L. Laak, A. L. Bartorelli, D. E. Cutlip, A. V Kaplan, and M. B. Leon. Dedicated Bifurcation Stent for the Treatment of Bifurcation Lesions Involving Large Side Branches: Outcomes From the Tryton Confirmatory Study. *JACC. Cardiovasc. Interv.* 9:1338–46, 2016.
14. Grundeken, M. J., C. Chiastra, W. Wu, J. J. Wykrzykowska, R. J. De Winter, G. Dubini, and F. Migliavacca. Differences in rotational positioning and subsequent distal main branch rewiring of the Tryton stent: An optical coherence tomography and computational study. *Catheter. Cardiovasc. Interv.* 0:1–10, 2018.
15. Grundeken, M. J., P. Généreux, J. J. Wykrzykowska, M. B. Leon, and P. W. Serruys. The Tryton Side Branch Stent. *EuroIntervention* 11 Suppl V:V145-6, 2015.
16. Grundeken, M. J., Y. Ishibashi, P. Généreux, L. LaSalle, J. Iqbal, J. J. Wykrzykowska, M.-A. Morel, J. G. Tijssen, R. J. de Winter, C. Girasis, H. M. Garcia-Garcia, Y. Onuma, M. B. Leon, and P. W. Serruys.

Inter-core lab variability in analyzing quantitative coronary angiography for bifurcation lesions: a post-hoc analysis of a randomized trial. *JACC Cardiovasc. Interv.* 8:305–314, 2015.

17. Grundeken, M. J., P. R. Stella, and J. J. Wykrzykowska. The Tryton Side Branch Stent™ for the treatment of coronary bifurcation lesions. *Expert Rev. Med. Devices* 10:707–16, 2013.

18. Grundeken, M. J., R. J. de Winter, and J. J. Wykrzykowska. Safety and efficacy of the Tryton Side Branch Stent™ for the treatment of coronary bifurcation lesions: an update. *Expert Rev. Med. Devices* 14:545–555, 2017.

19. Hariki, H., T. Shinke, H. Otake, J. Shite, M. Nakagawa, T. Inoue, T. Osue, M. Iwasaki, Y. Taniguchi, R. Nishio, N. Hiranuma, H. Kinutani, A. Konishi, and K. Hirata. Potential Benefit of Final Kissing Balloon Inflation After Single Stenting for the Treatment of Bifurcation Lesions. *Circ. J.* 77:1193–1201, 2013.

20. Holzapfel, G., G. Sommer, C. T. Gasser, and P. Regitnig. Determination of layer-specific mechanical properties of human coronary arteries with nonatherosclerotic intimal thickening and related constitutive modeling. *Am. J. Physiol. Heart Circ. Physiol.* 289:H2048–H2058, 2005.

21. Iannaccone, F., C. Chiastra, A. Karanasos, F. Migliavacca, F. J. H. Gijsen, P. Segers, P. Mortier, B. Verhegghe, G. Dubini, M. De Beule, E. Regar, and J. J. Wentzel. Impact of plaque type and side branch geometry on side branch compromise after provisional stent implantation: a simulation study. *EuroIntervention* 13:e236–e245, 2017.

22. Lassen, J. F., F. Burzotta, A. P. Banning, T. Lefèvre, O. Darremont, D. Hildick-Smith, A. Chieffo, M. Pan, N. R. Holm, Y. Louvard, and G. Stankovic. Percutaneous coronary intervention for the Left Main stem and other bifurcation lesions. The 12th consensus document from the European Bifurcation Club. *EuroIntervention* 13:1540–1553, 2017.

23. Lassen, J. F., N. R. Holm, A. Banning, F. Burzotta, T. Lefèvre, A. Chieffo, D. Hildick-Smith, Y. Louvard, and G. Stankovic. Percutaneous coronary intervention for coronary bifurcation disease: 11th consensus document from the European Bifurcation Club. *EuroIntervention* 12:38–46, 2016.

24. Medrano-Gracia, P., J. Ormiston, M. Webster, S. Beier, A. Young, C. Ellis, C. Wang, Ö. Smedby, and B. Cowan. A computational atlas of normal coronary artery anatomy. *EuroIntervention* 12:845–54, 2016.

25. Migliavacca, F., C. Chiastra, Y. S. Chatzizisis, and G. Dubini. Virtual bench testing to study coronary bifurcation stenting. *EuroIntervention* 11 Suppl V:V31–V34, 2015.

26. Morlacchi, S., C. Chiastra, E. Cutrì, P. Zunino, F. Burzotta, L. Formaggia, G. Dubini, and F. Migliavacca. Stent deformation, physical stress, and drug elution obtained with provisional stenting, conventional culotte and Tryton-based culotte to treat bifurcations: A virtual simulation study. *EuroIntervention* 9:1441–1453, 2014.

27. Morlacchi, S., C. Chiastra, D. Gastaldi, P. Giancarlo, G. Dubini, and F. Migliavacca. Sequential structural and fluid dynamic numerical simulations of a stented bifurcated coronary artery. *J. Biomech. Eng.* 133:121010, 2011.

28. Morlacchi, S., S. G. Colleoni, R. Cárdenes, C. Chiastra, J. L. Diez, I. Larrabide, and F. Migliavacca. Patient-specific simulations of stenting procedures in coronary bifurcations: Two clinical cases. *Med. Eng. Phys.* 35:, 2013.

29. Mortier, P., G. A. Holzapfel, M. De Beule, D. Van Loo, Y. Taeymans, P. Segers, P. Verdonck, and B. Verhegghe. A novel simulation strategy for stent insertion and deployment in curved coronary bifurcations: Comparison of three drug-eluting stents. *Ann. Biomed. Eng.* 38:88–99, 2010.

30. Ng, J., C. V. Bourantas, R. Torii, H. Y. Ang, E. Tenekecioglu, P. W. Serruys, and N. Foin. Local hemodynamic forces after stenting: implications on restenosis and thrombosis. *Arterioscler. Thromb. Vasc. Biol.* In press:, 2017.

31. Ormiston, J. A., G. Kassab, G. Finet, Y. S. Chatzizisis, N. Foin, T. J. Mickley, C. Chiastra, Y. Murasato, Y. Hikichi, J. J. Wentzel, O. Darremont, K. Iwasaki, T. Lefèvre, Y. Louvard, S. Beier, H. Hojeibane, A. Netravali, J. Wooton, B. Cowan, M. W. Webster, P. Medrano-Gracia, and G. Stankovic. Bench Testing and Coronary Artery Bifurcations: A Consensus Document from the European Bifurcation Club. *EuroIntervention* In press:, 2017.

32. Ormiston, J. A., M. W. I. Webster, B. Webber, J. T. Stewart, P. N. Ruygrok, and R. I. Hatrick. The "Crush" Technique for Coronary Artery Bifurcation Stenting: Insights From Micro-Computed Tomographic Imaging of Bench Deployments. *JACC Cardiovasc. Interv.* 1:351–357, 2008.

33. Ragkousis, G. E., N. Curzen, and N. W. Bressloff. Simulation of longitudinal stent deformation in a patient-specific coronary artery. *Med. Eng. Phys.* 36:467–476, 2014.

34. Schiavone, A., and L. G. Zhao. A study of balloon type, system constraint and artery constitutive model used in finite element simulation of stent deployment. *Mech. Adv. Mater. Mod. Process.* 1:1, 2015.

35. Scott, N. A. Restenosis following implantation of bare metal coronary stents: pathophysiology and pathways involved in the vascular response to injury. *Adv. Drug Deliv. Rev.* 58:358–76, 2006.

36. Torii, R., E. Tenekecioglu, C. Bourantas, E. Poon, V. Thondapu, F. Gijsen, Y. Sotomi, Y. Onuma, P. Barlis, A. S. H. Ooi, and P. W. Serruys. Five-year follow-up of underexpanded and overexpanded bioresorbable scaffolds: self-correction and impact on shear stress. *EuroIntervention* 12:2158–2159, 2017.

37. Tyczynski, P., G. Ferrante, N. Kukreja, C. Moreno-Ambroj, P. Barlis, N. Ramasami, R. De Silva, K. Beatt, and C. Di Mario. Optical coherence tomography assessment of a new dedicated bifurcation stent. *EuroIntervention* 5:544–51, 2009.

Table

Table 1. Quantitative biomechanical results obtained for the three investigated cases after virtual stenting.

Case	Distal angle change [°]	SB ostial area stenosis [%]	Stent malapposition [%]	Arterial wall peak stress [MPa]
'Proximal'	-4.8	74.3	16.3	2.20
'Recommended'	-6.9	44.8	9.9	0.37
'Distal'	-8.4	51.5	8.5	0.71

Figures

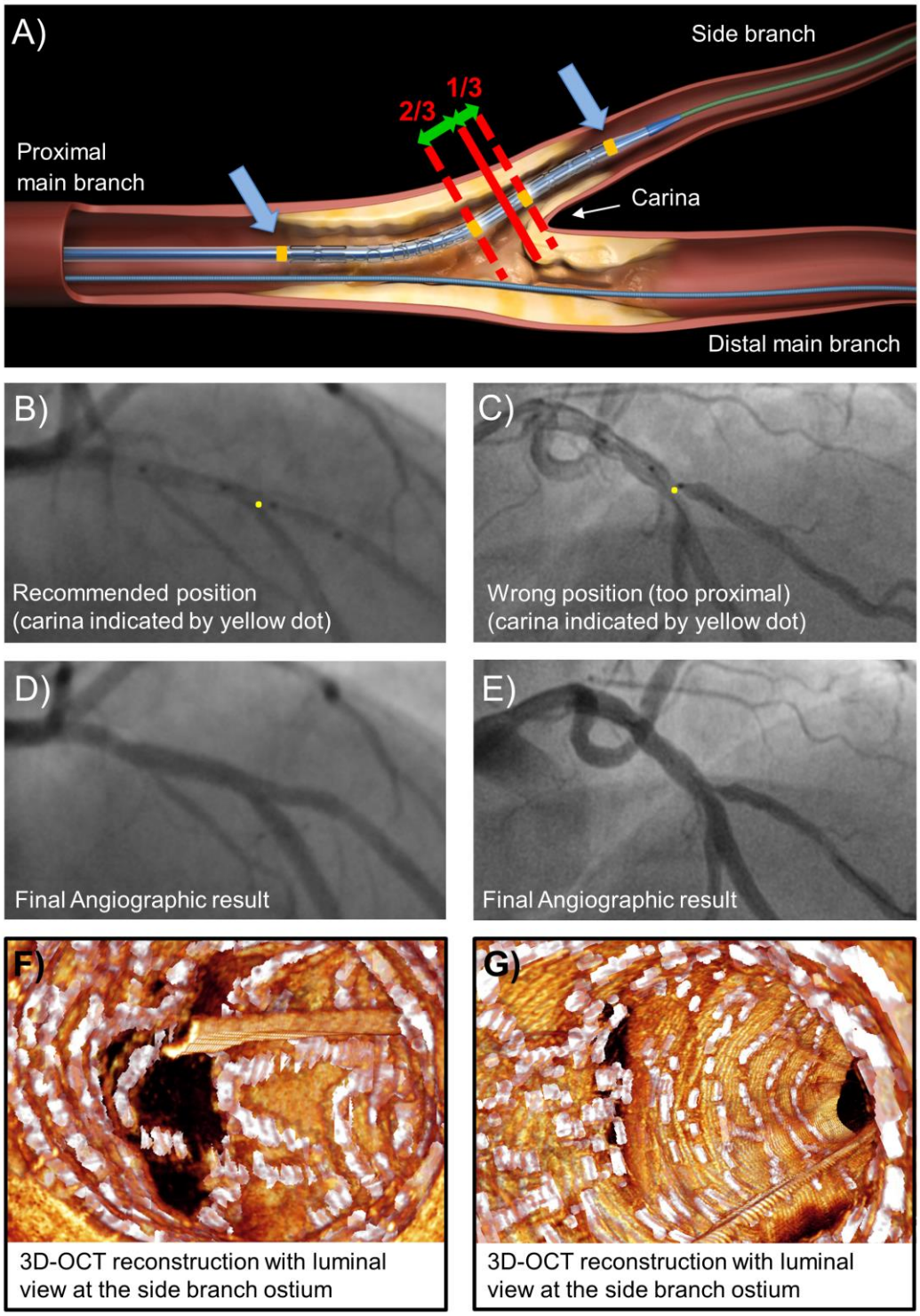

Figure 1. The Tryton Side Branch stent (Tryton Medical, Inc., USA). A) Correct positioning of the Tryon stent according to the manufacturer recommendations: the stent should be deployed so that the

carina is positioned 1/3 the distance from the distal middle marker (markers indicated by orange boxes), as indicated by the red lines in the drawing (http://www.trytonmedical.com). B) Clinical example of 'recommended' Tryton stent positioning. Note that the carina (indicated by yellow dot) is positioned 1/3 distance from the distal middle marker. C) Clinical example of incorrect Tryton stent positioning: the Tryton stent is positioned too proximally, with the carina placed in one line with the distal middle marker. D) Final angiogram of the correct positioning shows an excellent result. E) In this example of too proximal positioning, final angiographic result was poor with pinching of the ostium. F) 3D optical coherence tomography (OCT) reconstruction from a main branch pullback of the same case example as reported in B) and D) showing the luminal view at the side branch ostium. G) 3D-OCT reconstruction from a main branch pullback of the case example reported in C) and E) showing a small, pinched side branch ostium.

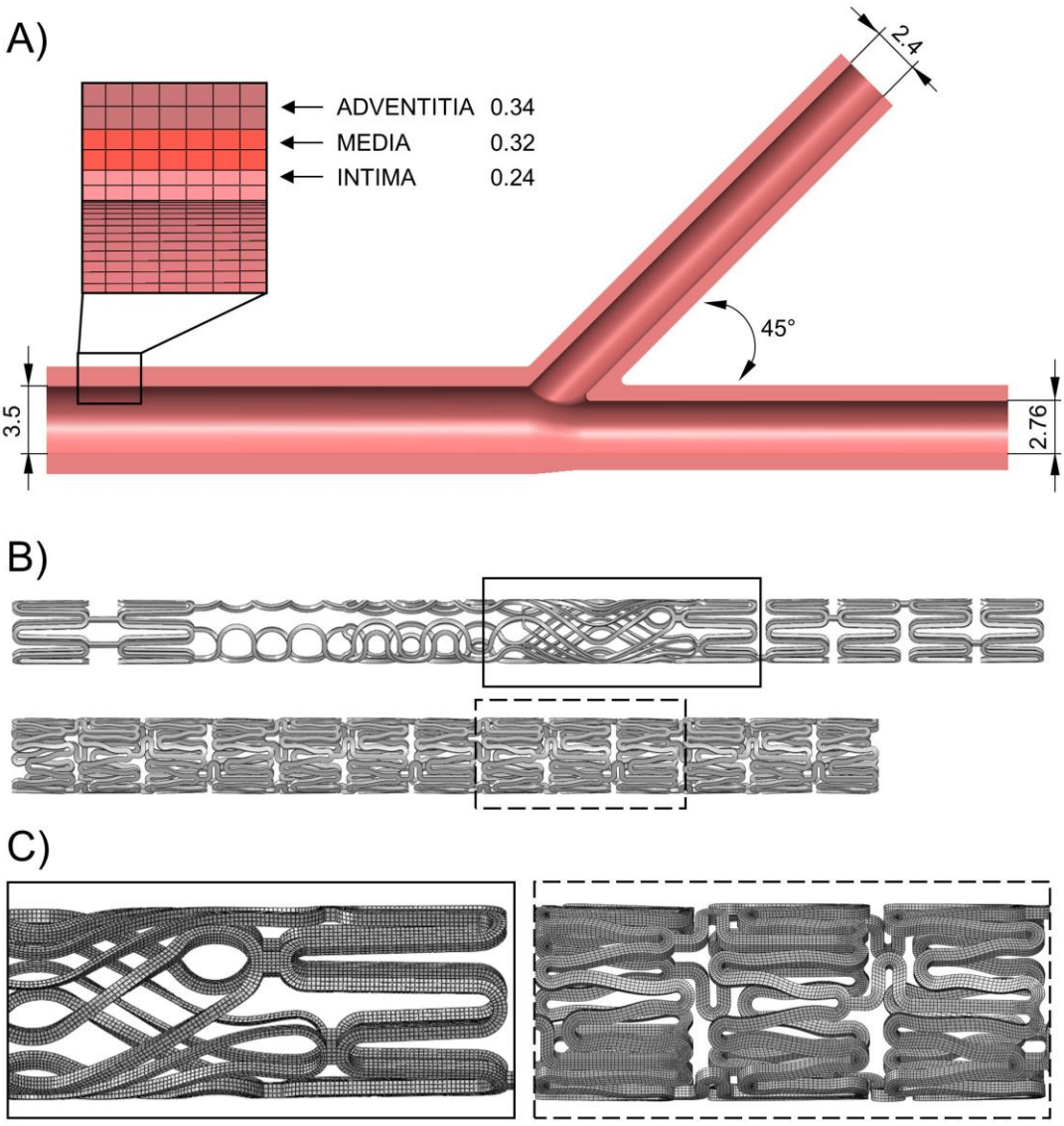

Figure 2. A) Geometrical model of the left anterior descending / first diagonal branch coronary bifurcation. A detail of the mesh of the arterial wall with the intima, media, and adventitia layers is shown. All measures are in mm. B) Geometrical models of (top) the Tryton stent (Tryton Medical, Inc., USA) and (bottom) the Xience V stent (Abbott Laboratories, USA) in their crimped configuration. C) Details of the mesh of (left) the Tryton and (right) the Xience V stent models.

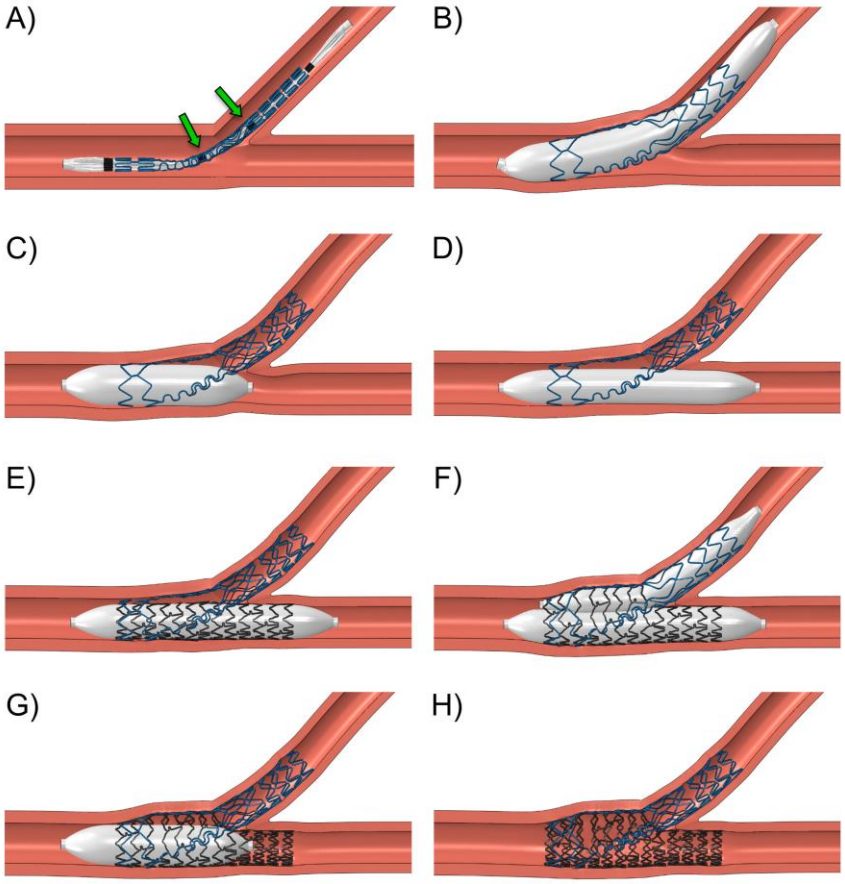

Figure 3. Simulation of the deployment sequence of the Tryton stent (Tryton Medical, Inc., USA) in a coronary bifurcation model: A) Insertion of a 2.5, 3.5 x 19 mm Tryton stent in the bifurcation side branch. B) Expansion of the Tryton stent. C) Proximal optimization technique with the expansion of a 3.5x9 mm NC Sprinter RX balloon (Medtronic, USA) in the proximal main branch. D) Opening of the main branch access with the expansion of a 3x15 mm NC Sprinter RX balloon. E) Expansion of a 3x15 mm Xience V stent (Abbott Laboratories, USA) in the main branch. F) Kissing balloon inflation with the simultaneous expansion of a 2.5x15 mm and 3x15 mm NC Sprinter RX balloon in the side branch and main branch, respectively. G) Proximal optimization technique with the expansion of a 3.5x9 mm NC Sprinter RX balloon in the proximal main branch. H) Final geometry after stent recoil. The 'recommended' case was used as example to show the steps of the Tryton stent deployment sequence.

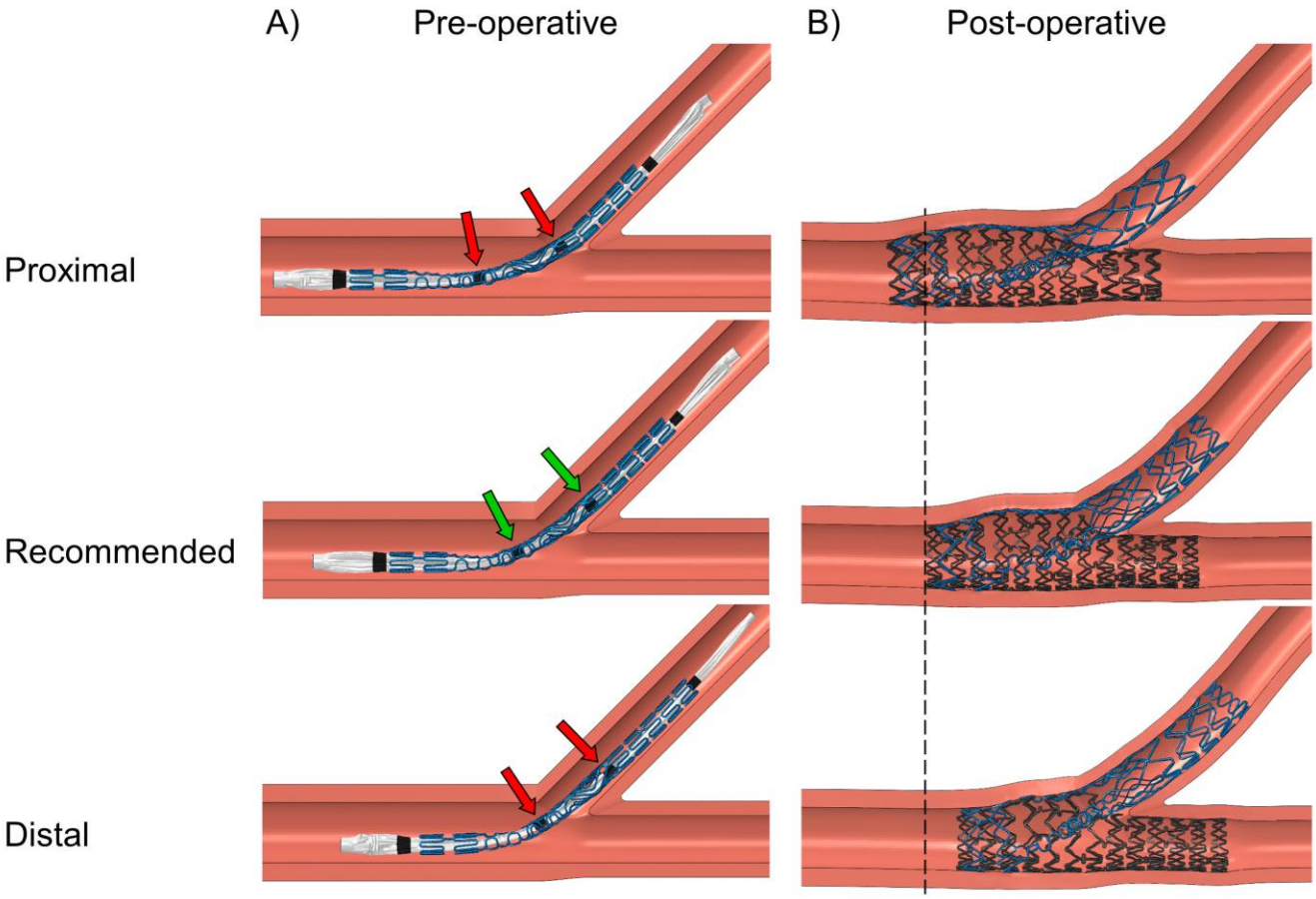

Figure 4. The three different cases under investigation: (top) 'proximal', (center) 'recommended', and (bottom) 'distal' Tryton stent positioning. A) Pre-operative vessel geometry with the insertion of the Tryton stent in the side branch. The arrows indicate the two middle radio-opaque markers that are used by the interventional cardiologist to place the stent in the side branch. B) Post-operative stented geometry obtained at the end of the Tryton stent deployment sequence.

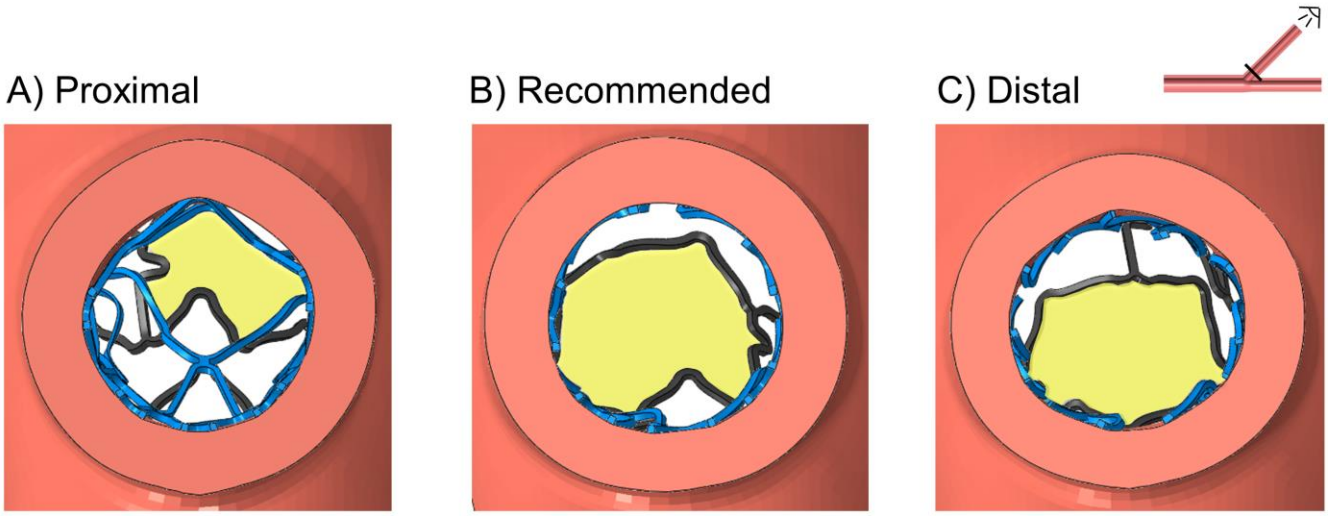

Figure 5. Cross-sectional view of the side branch ostium of the three investigated cases: (A) 'proximal', (B) 'recommended', and (C) 'distal' Tryton stent positioning. The side branch ostial area stenosis is highlighted in yellow.

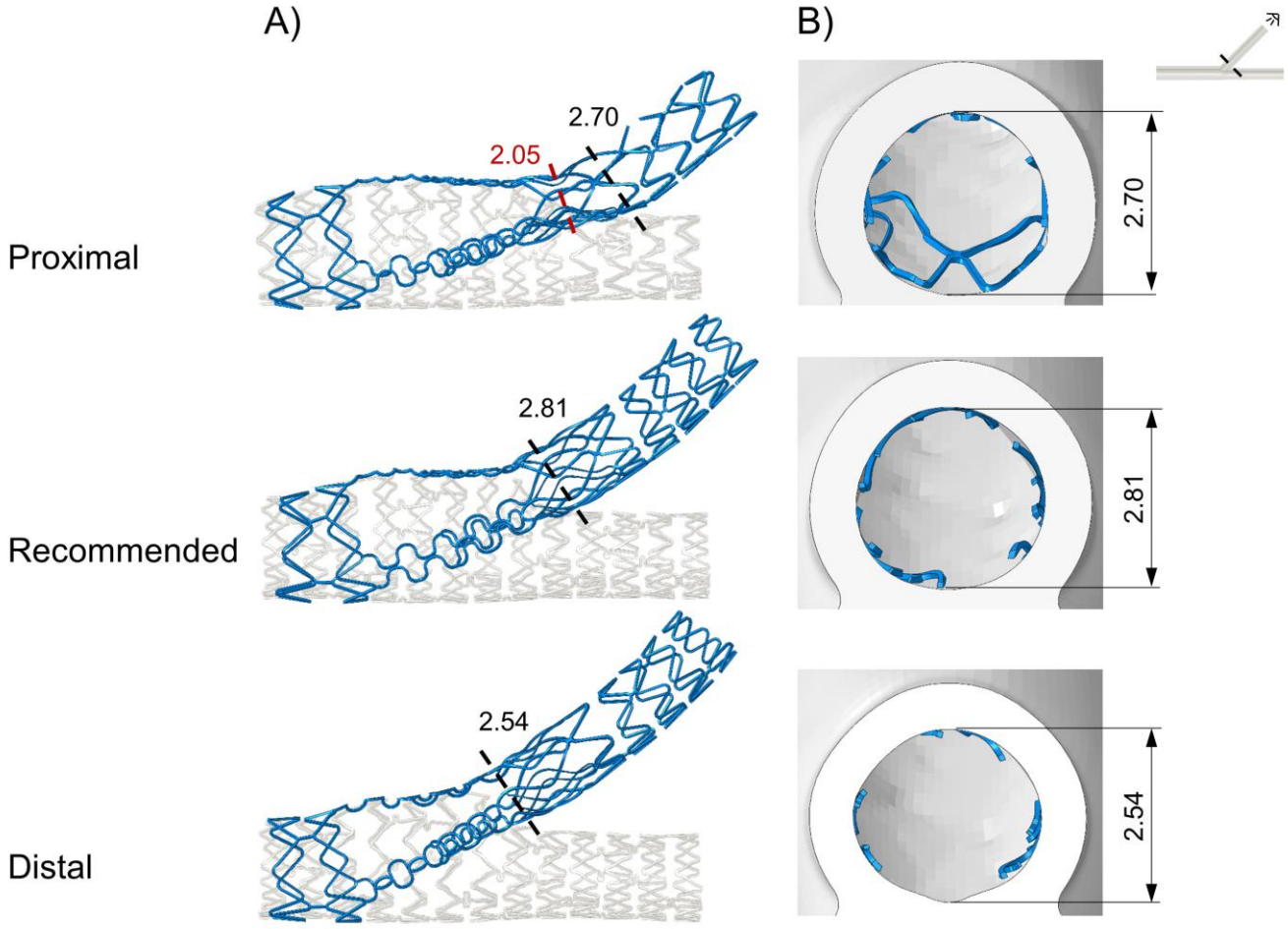

Figure 6. Tryton stent diameter at the side branch ostium for the three different cases under investigation: (top) 'proximal', (center) 'recommended', and (bottom) 'distal' Tryton stent positioning. A) Lateral view of the two virtually implanted stents. B) Cross-sectional view of the side branch ostium. Only the Tryton stent is shown. All measures are in mm.

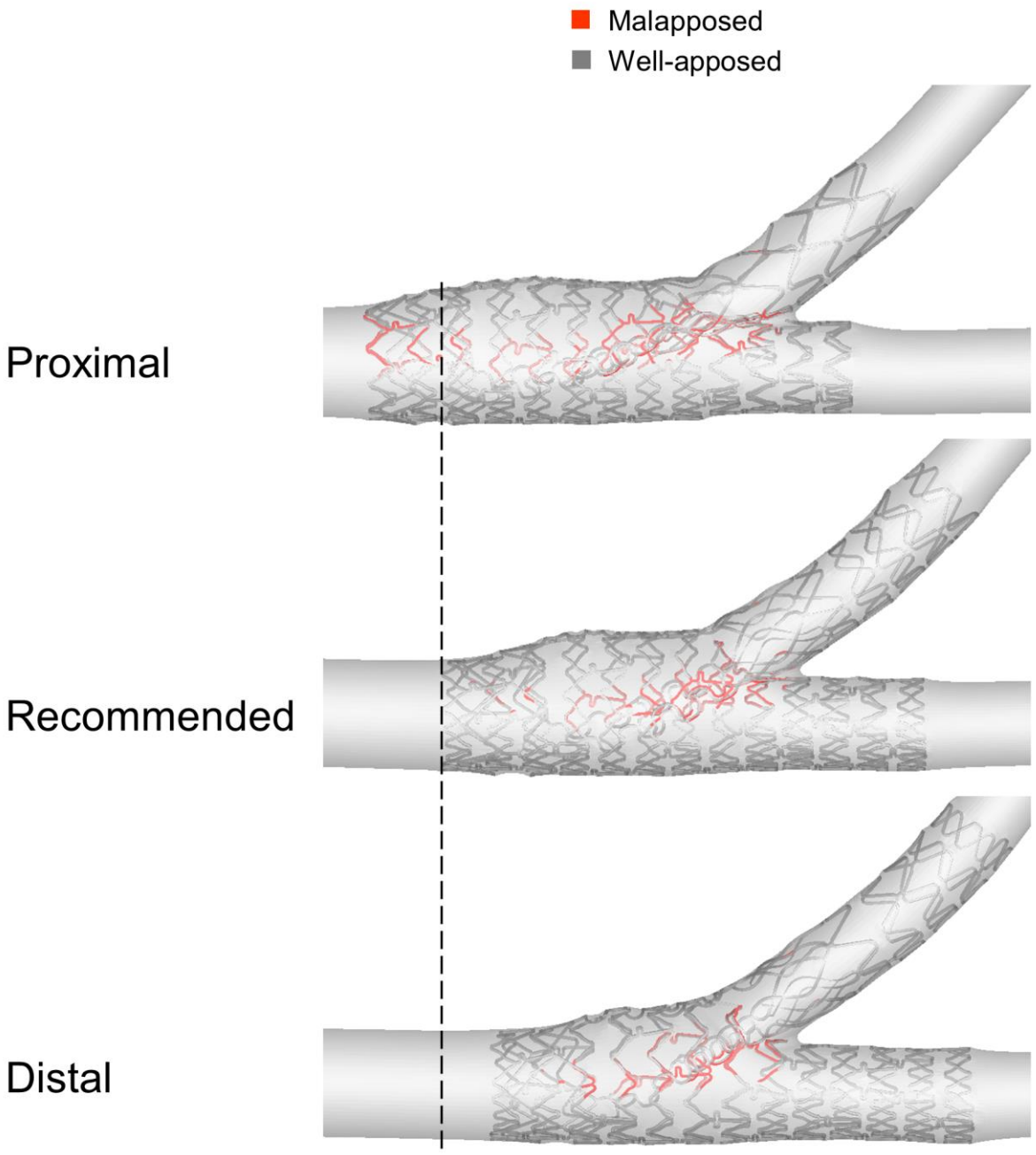

Figure 7. Quantification of stent malapposition for the three different cases under investigation: (top) 'proximal', (center) 'recommended', and (bottom) 'distal' Tryton stent positioning. Malapposed stent struts are colored in red.

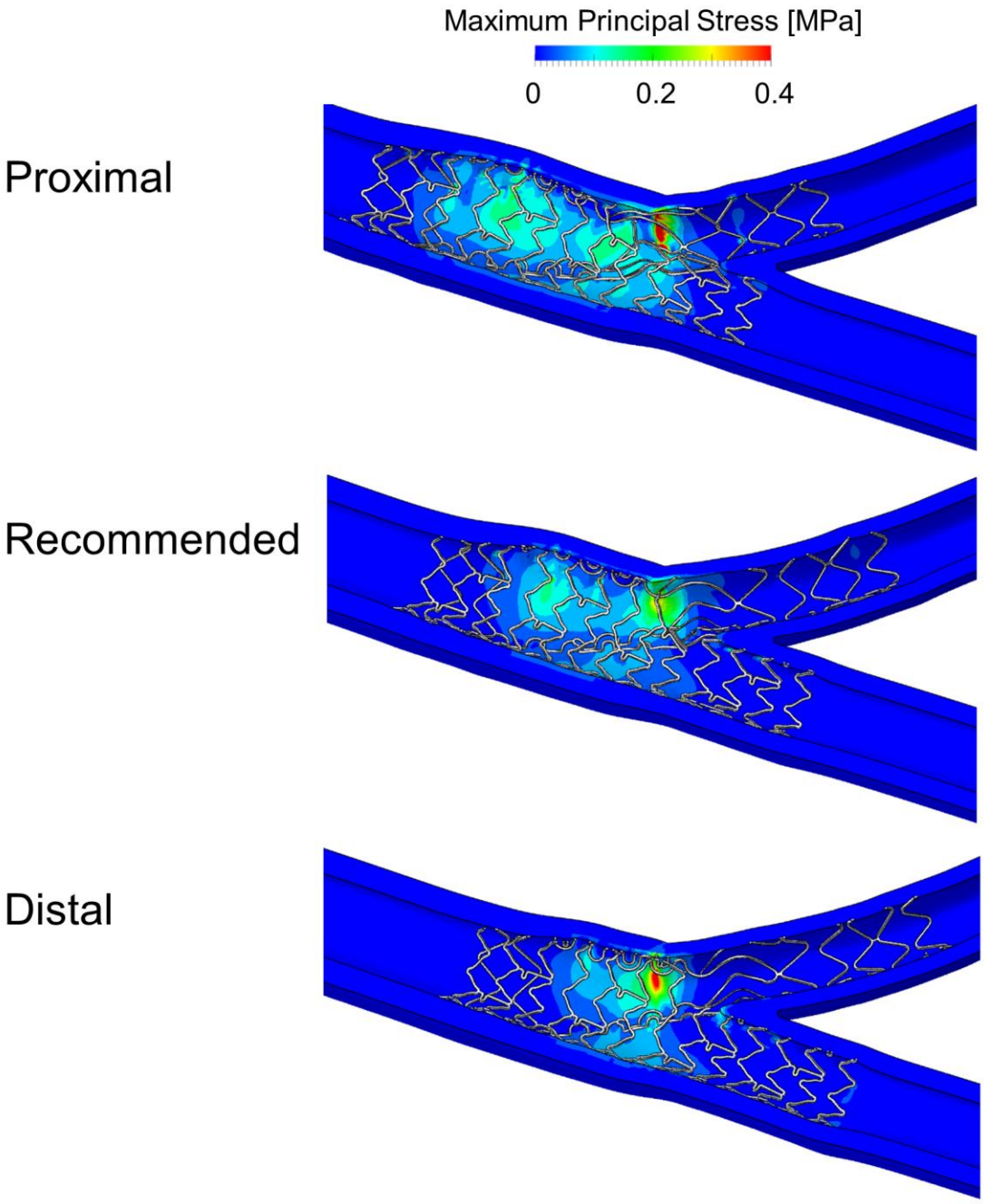

Figure 8. Contour maps of maximum principal stress in the arterial wall for the three different cases under investigation: (top) 'proximal', (center) 'recommended', and (bottom) 'distal' Tryton stent positioning.